ONLINE METHODS

Study population. The medical ethical review committees of all participating study centers approved this study. All study subjects gave informed consent. We enrolled 944 unrelated German individuals with a diagnosis of nonalcoholic chronic pancreatitis and 465 subjects with alcohol-related chronic pancreatitis. In the replication study, we investigated 600 unrelated subjects with nonalcoholic chronic pancreatitis originating from France (n = 456), the Czech Republic (n = 21) and Poland (n = 123). In addition, we investigated unrelated subjects affected with nonalcoholic chronic pancreatitis from India (n = 230) and Japan (n = 247). The diagnosis of chronic pancreatitis was based on two or more of the following findings: presence of a typical history of recurrent pancreatitis, pancreatic calcifications and/or pancreatic ductal irregularities revealed by endoscopic retrograde pancreaticography or by magnetic resonance imaging of the pancreas, and/or pathological sonographic findings. Alcoholic chronic pancreatitis was diagnosed in subjects who consumed more than 60 g (females) or 80 g (males) of ethanol per day for more than 2 years. Control subjects were recruited from Germany (n = 3,938), France (n = 2,000), the Czech Republic (n = 235), Poland (n = 197), India (n = 264) and Japan (n = 341).

Mutation screening. We designed primers complementary to intronic sequences flanking *CPA1* exons on the basis of the published nucleotide sequence (GenBank NT_007933.15) (**Supplementary Table 2**). After PCR amplification, the entire coding region and the exon-intron boundaries were sequenced. All mutations were confirmed with a second independent PCR reaction. In the German laboratories, we performed PCR using 0.75 U AmpliTaq Gold polymerase (Perkin Elmer), 400 µmol/l deoxynucleoside triphosphates and 0.1 µmol/l primers in a total volume of 25 µl. The cycle conditions were as follows: initial denaturation for 12 min at 95 °C; 48 cycles of 20 s denaturation at 95 °C, 40 s annealing at 64 °C and 90 s primer extension at 72 °C; and a final extension step for 2 min at 72 °C. PCR products were digested with Antarctic phosphatase (New England Biolabs) or shrimp alkaline phosphatase (USB) and exonuclease I (New England Biolabs). Cycle sequencing was performed using BigDye terminator mix (Applied Biosystems) with a 56 °C annealing temperature. The reaction products were purified with ethanol precipitation and loaded onto an ABI 3730 or ABI 3100-Avant fluorescence sequencer (Applied Biosystems).

Functional characterization of CPA1 variants. We investigated the functional consequences of *CPA1* alterations by transient transfection of HEK 293T cells (#Q401, GenHunter) with wild-type and mutant constructs and analyzing the conditioned medium for the amount of proCPA1 protein constitutively secreted using densitometry of stained gels and CPA1 activity after activation with trypsin and CTRC.

Expression plasmids, mutagenesis and adenoviruses. Construction of the pcDNA3.1(-) human *CPA1* expression plasmid has been reported previously[12]. The coding DNA in this plasmid was derived from IMAGE clone #3949850 (GenBank accession BC005279), which contains a c.827A>G (p.His276Arg) alteration. This error was corrected by back mutating Arg276 to histidine. *CPA1* mutants were created by PCR mutagenesis and ligated into the pcDNA3.1(-) expression plasmid. Recombinant adenoviruses carrying wild-type *CPA1* or the p.Asn256Lys mutant were generated by Viraquest. Details regarding the construction of the *CPA1* splice-site and duplication mutant expression plasmids are provided in the **Supplementary Note**.

Cell culture and transfection. HEK 293T cells were cultured in six-well tissue culture plates (1.5×10^6 cells per well) in DMEM (Invitrogen) supplemented with 10% fetal bovine serum, 4 mM glutamine and 1% penicillin and streptomycin at 37 °C. Transfections were carried out at 90% confluence using 10 µl Lipofectamine 2000 (Invitrogen) and 4 µg expression plasmids in a final volume of 2 ml DMEM. After overnight incubation, cells were washed, and the transfection medium was replaced with 2 ml OPTI-MEM I Reduced Serum Medium (Invitrogen). The conditioned OPTI-MEM media were harvested after 48 h of incubation. AR42J rat pancreatic acinar cells (American Type Culture Collection #CRL-1492) were maintained in DMEM supplemented with 20% fetal bovine serum, 4 mM glutamine and 1% penicillin and streptomycin at 37 °C. Before transfection, cells were plated in six-well plates (10^6 cells per well) and grown in the presence of a 100 nM concentration of dexamethasone for 48 h to induce differentiation. Infections with adenoviruses were performed using 4×10^7 pfu per ml of the final adenovirus concentrations in a total volume of 1 ml OPTI-MEM in the presence of dexamethasone (100 nM final concentration).

CPA1 activity assay. The enzymatic activity of CPA1 was determined after activation with trypsin and CTRC using the N-[4-methoxyphenylazoformyl]-L-phenylalanine substrate[17] with minor modifications of our previously published conditions[12]. The CPA1 activity measured in the conditioned medium of transfected cells is referred to as the 'apparent activity' and reflects the combined effects of the variants on the secreted amounts of proCPA1, the proteolytic degradation during activation and the catalytic activity of the activated CPA1. To activate proCPA1, an aliquot (20 µl) of the conditioned medium was supplemented with 0.1 M Tris-HCl (pH 8.0), 1 mM $CaCl_2$, 0.05% Tween 20, 100 nM human cationic trypsin and 50 nM human CTRC (final concentrations in a final volume of 40 µl) and incubated at 37 °C for 60 min. CPA1 activity was then measured by adding 50 µl assay buffer (0.1 M Tris-HCl (pH 8.0), 1 mM $CaCl_2$ and 0.05% Tween 20) and 10 µl substrate (final concentration of 60 µM) to the activation mix. The decrease in absorbance was followed at 350 nm for 2 min. Rates of substrate cleavage were calculated from fits to the initial linear portion of the curves and are expressed as a percentage of the wild-type rate, which was set to 100%. The wild-type activity corresponded to 116 ± 34 milliOD min^{-1} (average ± s.d.), which equals a 262 ± 77 nM s^{-1} substrate cleavage rate.

Measurement of proCPA1 secretion. Secreted amounts of proCPA1 protein in the conditioned medium were determined by SDS-PAGE and densitometry. An aliquot (200 µl) of the medium was precipitated with trichloroacetic acid (10% final concentration), the precipitate was recovered by centrifugation, dissolved in 20 µl Laemmli sample buffer containing 100 mM dithiothreitol (DTT) (final concentration) and heat denatured at 95 °C for 5 min. Electrophoretic separation was performed on 15% SDS-PAGE mini gels in standard Tris-glycine buffer, and gels were stained with Brilliant Blue R-250. Quantification of bands was carried out with the GelDocXR+ gel documentation system and Image Lab 3.0 software (Bio-Rad).

Measurement of endoplasmic reticulum stress. To study endoplasmic reticulum stress, we generated recombinant adenoviruses carrying either wild-type *proCPA1* or the p.Asn256Lys mutant, infected AR42J rat pancreatic acinar cells (#CRL-1492, American Type Culture Collection (ATCC)) with these viruses and measured endoplasmic reticulum stress markers as described below.

RT-PCR analysis and real-time PCR. Total RNA was extracted from AR42J cell lysates using an RNeasy mini kit (Qiagen). RNA was reverse transcribed using the High Capacity cDNA Reverse Transcription Kit (Applied Biosystems). *Xbp1* (encoding X-box binding protein 1) splicing was studied by PCR using a primer set that flanked the spliced region and amplified both the spliced and unspliced forms (**Supplementary Table 3**). PCR was carried out using the *Taq* DNA Polymerase kit (Qiagen) with the following conditions: 10 min initial denaturation at 95 °C followed by 35 cycles of 30 s denaturation at 95 °C, 30 s annealing at 52 °C, 30 s extension at 72 °C and a final extension at 72 °C for 5 min. The PCR products were resolved on 2% agarose gels and stained with ethidium bromide. Quantification of mRNA expression was performed by real-time PCR (7500 Real Time PCR System, Applied Biosystems). *Xbp1* expression was measured with SYBR Green (PCR Master Mix, Applied Biosystems) using different primer sets for the spliced, unspliced and total mRNA (**Supplementary Table 3**). Levels of *Hspa5* (encoding the immunoglobulin-binding protein BiP) and *Calr* (encoding calreticulin) mRNA were determined using TaqMan primers (rat *Hspa5*, Rn00565250_m1; rat *Calr*, Rn00574451_m1) with TaqMan Universal PCR Mastermix (Applied Biosystems). Real-time PCR conditions were as follows: 2 min equilibration at 50 °C, 10 min denaturation and enzyme activation at 95 °C followed by 40 two-step cycles of 15 s at 95 °C and 60 s at 60 °C. Gene expression was quantified using the comparative C_T method ($\Delta\Delta C_T$ method). Threshold cycle (C_T) values were determined using the 7500 System Sequence Detection Software 1.3.

Expression levels of target genes were first normalized to the *Gapdh* internal control gene (ΔC_T) and then to the expression levels measured in cells infected with empty adenovirus ($\Delta\Delta C_T$). Results were expressed as fold changes calculated with the formula $2^{-\Delta\Delta CT}$.

Statistics. The significance of the differences between mutation frequencies in affected individuals and controls was tested by two-tailed Fisher's exact test. Additional ORs were calculated using SAS/STAT software (v 9.1) and GraphPad Prism (v 4.03).

17. Mock, W.L., Liu, Y. & Stanford, D.J. Arazoformyl peptide surrogates as spectrophotometric kinetic assay substrates for carboxypeptidase A. *Anal. Biochem.* **239**, 218–222 (1996).

RESEARCH ARTICLE

AMERICAN JOURNAL OF medical genetics PART A

Clinical Consequences in Truncating Mutations in Exon 34 of *NOTCH2*: Report of Six Patients With Hajdu–Cheney Syndrome and a Patient With Serpentine Fibula Polycystic Kidney Syndrome

Yoko Narumi,[1]* Byung-Joo Min,[2] Kenji Shimizu,[3] Itsuro Kazukawa,[4] Kiyoko Sameshima,[5] Koichi Nakamura,[6] Tomoki Kosho,[1] Yumie Rhee,[7] Yoon-Sok Chung,[8] Ok-Hwa Kim,[9] Yoshimitsu Fukushima,[1] Woong-Yang Park,[2] and Gen Nishimura[10]

[1]Department of Medical Genetics, Shinshu University School of Medicine, Matsumoto, Japan

[2]Departments of Biomedical Sciences, Seoul National University College of Medicine, Seoul, Korea

[3]Division of Medical Genetics, Saitama Children's Medical Center, Saitama, Japan

[4]Division of Endocrinology, Chiba Children's Hospital, Chiba, Japan

[5]Division of Medical Genetics, Gunma Children's Medical Center, Shibukawa, Japan

[6]Department of Orthopedics, Shinshu University School of Medicine, Matsumoto, Japan

[7]Department of Internal Medicine, Endocrine Research Institute, Yonsei University College of Medicine, Seoul, Korea

[8]Department of Endocrinology and Metabolism, Ajou University School of Medicine, Suwon, Korea

[9]Department of Radiology, Ajou University School of Medicine, Suwon, Korea

[10]Department of Pediatric Imaging, Tokyo Metropolitan Children's Medical Center, Tokyo, Japan

Manuscript Received: 3 March 2012; Manuscript Accepted: 11 October 2012

How to Cite this Article:
Narumi Y, Min B-J, Shimizu K, Kazukawa I, Sameshima K, Nakamura K, Kosho T, Rhee Y, Chung YS, OH Kim, Fukushima Y, Park WY, Nishimura G. 2013. Clinical consequences in truncating mutations in exon 34 of *NOTCH2*: Report of six patients with Hajdu–Cheney syndrome and a patient with serpentine fibula polycystic kidney syndrome.
Am J Med Genet Part A 161A:518–526.

It is debatable whether Hajdu–Cheney syndrome (HCS) and serpentine fibula-polycystic kidney syndrome (SFPKS) represent a single clinical entity with a variable degree of expression or two different entities, because both disorders share common clinical and radiological manifestations, including similar craniofacial characteristics, and defective bone mineralization. Since it was shown that heterozygous truncating mutations in *NOTCH2* are responsible for both HCS and SFPKS, 37 patients with HCS and four patients with SFPKS are reported. To elucidate the clinical consequences of *NOTCH2* mutations, we present detailed clinical information for seven patients with truncating mutations in exon 34 of *NOTCH2*, six with HCS and one with SFPKS. In addition, we review all the reported patients whose clinical manifestations are available. We found 13 manifestations including craniofacial features, acroosteolysis, Wormian bones, and osteoporosis in >75% of *NOTCH2*-positive patients. Acroosteolysis was observed in two patients with SFPKS and bowing fibulae were found in two patients with HCS. These clinical and molecular data would support the notion that HCS and SFPKS are a single disorder.

Key words: Hajdu–Cheney syndrome; serpentine fibula-polycystic kidney syndrome; NOTCH2; osteolysis; osteoporosis

Additional supporting information may be found in the online version of this article.

Grant sponsor: Research on Grant-in-Aid, Ministry of Education, Culture, Sports, Science and technology, Japan; Grant numbers: 22790972, 24791844; Grant sponsor: The Korea Healthcare Technology R&D Project, Ministry for Health, Welfare and Family Affairs, Republic of Korea; Grant number: A080588.

Yoko Narumi, Byung-Joo Min, and Woong-Yang Park contributed equally to this work.

*Correspondence to:
Yoko Narumi, M.D., Ph.D., Department of Medical Genetics, Shinshu University School of Medicine, 3-1-1 Asahi, Matsumoto 390-8621, Japan.
E-mail: ynarumi@shinshu-u.ac.jp

Article first published online in Wiley Online Library (wileyonlinelibrary.com): 7 February 2013
DOI 10.1002/ajmg.a.35772

INTRODUCTION

Hajdu–Cheney syndrome (HCS) [OMIM#102500] is a rare autosomal dominant disorder, which is characterized by short stature, craniofacial anomalies, abnormal dentition, joint hypermobility, hearing impairment, defective bone mineralization, and progressive bone resorption, including progressive osteoporosis, multiple Wormian bones, progressive basilar invagination, and acroosteolysis [Brennan and Pauli, 2001]. HCS shares common manifestations with serpentine fibula-polycystic kidney syndrome (SFPKS) [OMIM#600330] which is characterized by facial dysmorphism that resembles HCS, short stature, polycystic kidneys, hearing impairment, bowed forearms, and elongated and S-shaped fibulae [Exner, 1988; Majewski et al., 1993]. It debatable whether HCS and SFPKS represent a single clinical entity with a variable degree of expression or two different entities [Kaplan et al., 1995; Ramos et al., 1998; Currarino, 2009; Takatani et al., 2009].

It has recently been demonstrated that heterozygous truncating mutations in *NOTCH2* are responsible for both HCS and SFPKS. To date, 37 patients with HCS and four patients with SFPKS have been reported with *NOTCH2* mutations [Isidor et al., 2011a,b; Majewski et al., 2011; Simpson et al., 2011; Gray et al., 2012]. *NOTCH2* encodes a single-pass transmembrane protein from the NOTCH receptor family (NOTCH1–NOTCH4 in mammals). It is intriguing that both HCS and SFPKS are caused by nonsense or frameshift mutations in the proline-glutamic acid-serine-threonine-rich (PEST) domain of *NOTCH2*. The PEST domain is essential for the proteasomal degradation of the Notch intracellular domain (NICD) and is located at the C terminus of the receptor. It is assumed that HCS or SFPKS-related *NOTCH2* mutations escape nonsense-mediated mRNA decay and cause gain-of-function effects [Simpson et al., 2011]. In murine models, the activation of Notch signaling arrests the commitment of pluripotent precursors to the osteoblastic lineage, and suppresses osteoblast differentiation [Zanotti and Canalis, 2012].

To elucidate clinical consequences of truncating mutations in exon 34 of *NOTCH2*, we present detailed clinical information of seven patients with *NOTCH2* mutations, six with HCS and one with SFPKS and clinical review of all reported patients whose clinical manifestations are available. This investigation may help us to decide whether the two conditions are distinct disorders or a single disorder.

CLINICAL REPORTS

Patient 1

Patient 1, a Japanese girl now 2 years of age, was the second child born to healthy nonconsanguineous parents. Bowed femurs were detected by prenatal ultrasonography at 25 weeks of gestation. She was delivered by cesarean at 37 weeks of gestation. Her birth length was 46 cm (10th centile of Japanese girls), weight 3,114 g (50th–75th centile of Japanese girls), occipital frontal circumference (OFC) of 35.5 cm (>97th centile of Japansese girl). Her apgar score was 3 at 1 min, and she received oxygen inhalation therapy because of respiratory insufficiency. Radiographs detected bowing of the femur, tibiae, and fibulae; deformation of the radii and ulnae; and a fracture line in the right femur. Echocardiography indicated a patent ductus arteriosus and trivial aortic regurgitation. Abdominal ultrasonography revealed bilateral polycystic kidneys.

At 3 months, she presented with a large anterior fontanelle ($3.5 \times 3.5\ cm^2$), diastasis of the sagittal suture, arched eyebrows, shallow orbit, mild proptosis, hypertelorism, broad nasal bridge, long philtrum, thin upper lip vermilion, micrognathia (Fig. 1A), a bifid uvula, and a short neck. Hearing impairment was detected with a threshold of 60 dB in the auditory brainstem response (ABR). A fiber optic laryngoscope detected laryngomalacia. Cranial magnetic resonance imaging (MRI) showed mild hydorocephalus at 10 months of age. The radiological findings included Wormian bones, patent cranial sutures, delayed calvarial ossification (Fig. 2A), generalized osteopenia with mild scoliosis (Fig. 3A), and acroosteolysis of both hands (Fig. 4A), which was first identified at 1 year and 6 months of age. Mildly bowed tibiae and serpentine fibulae were observed (Fig. 4B,C). The right fibula and left fifth metacarpal was fractured at 2 years of age. At 2 years and 8 months, her height was 81.2 cm (<3rd centile), weight 9.8 kg (<3rd centile), and OFC 49.5 cm (75th–90th centile). She showed developmental retardation with a developmental quotient (DQ) of 52 at 2 years and 7 months, and she was fed by a tube until 2 years and 4 months because of poor feeding.

Patient 2

Patient 2 was a Japanese girl who is now 14 years of age. Part of her medical history has been reported previously [Takatani et al., 2009]. At birth, she presented with exophthalmos, depression of the nasal tip, long philtrum, low-set ears, micrognathia, and a patent ductus arteriosus. Subsequently, she was found to have a submucous cleft palate, conductive hearing impairment, early loss of teeth, hydrocephalus, and platybasia. At 5 months of age, she was noted with optic nerve abnormal whiteness. She was diagnosed with bilateral optic nerve atrophy secondary to hydrocephalus. Renal ultrasonography detected normal kidneys. She experienced a left ulna and radius fracture at 6 years of age and two lumbar vertebral fractures at 13 years of age. Radiological findings including mild metaphyseal undermodeling of the long bones, bowing of the fibulae and ulnae, dislocation of the elbow joints, and a pseudofracture of the right fibula were reported previously. In addition, radiographs detected multiple Wormian bones, bathrocephaly (Fig. 2B), acroosteolysis of the distal phalanges (Fig. 4D), and generalized osteoporosis with vertebral compression fractures and thoracolumbar kyphosis (Fig. 3B). At 9 years of age, she reported headache, emesis, and gait difficulties. Cranial MRI showed platybasia with basilar invagination, progressive hydrocephalus, medullary kinking, and syringomyelia. She underwent surgery comprising a fenestration in the floor of the third ventricle, foramen magnum augmentation, and a ventriculoperitoneal shunt to improve symptoms. She exhibited developmental retardation with a DQ of 64 at 2 years and 6 months of age. At 14 years of age, her height was 126 cm (<3rd centile of Japanese girls) and her weight was 27 kg (<3rd centile of Japanese girls). She currently uses a wheelchair because of gait difficulties.

FIG. 1. Facial photographs. Patient 1 with arched eyebrows at 3 months of age (A). Patient 3 at 1 month; synophyrys was not noted (B), but recognized at 2 years (C). Patient 4 showed synophyrys in infancy (D), 3 years of age (E), and coarse hair and skins at 31 years of age (F).

Patient 3

Patient 3, a Japanese girl who is now 2 years of age, was the first child born to healthy nonconsanguineous parents. Pregnancy was associated with polyhydramnios. Prenatal ultrasonography revealed a hypoplastic left heart. She was born at 37 weeks of gestation. Her birth length was 47 cm (25th centile of Japanese girls), weight 2,952 g (50th centile of Japanese girls), and OFC 34.5 cm (90th centile of Japanese girls). Cardiac ultrasonography at birth showed hypoplastic left ventricle, subaortic stenosis, coarctation of aorta, and patent ductus arteriosus. She showed pulmonary hypertension and required oxygen therapy. At 30 months of age, her height was 81.2 cm (<3rd centile), weight 9.8 kg (<3rd centile), and OFC 48.6 cm (75th centile). Her left ventricle formation was improved with age. However, she presented with severe pulmonary hypertension and coarctation of aorta. She had a facial dysmorphism and rounded nails (Fig. 1B,C). Radiographs detected Wormian bones in the lambdoidal sutures (Fig. 2C) and mild bowing of the tibiae was evident. However, neither acroosteolysis nor osteoporosis was apparent (Figs. 3C and 4E,F) and polycystic kidney was not detected by renal ultrasonography. She exhibited normal development.

Patient 4

Patient 4 is now a 31-year-old Japanese woman. Her birth weight was 3,900 g (>97th centile of Japanese females). In her childhood, she presented with thick eyebrows, a short nose, a long philtrum, and micrognathia (Fig. 1D,E). Her development was normal. In her early elementary school years, she presented short fingers with rounded tips. The delayed loss of primary teeth and malposition of teeth were also observed. At 14 years of age, hallux valgus and distal interphalangeal joint contracture were noted and chronic back pain and stiff shoulders were also observed. She has had irregular menstrual cycle from menarche; thus, was suspected to have anovulomenorrhea, but she became pregnant and delivered a healthy son at age 28 years of age.

At 30 years of age, her height was 156 cm (50th centile) and weight 51 kg (50th centile). She had distinctive facial features

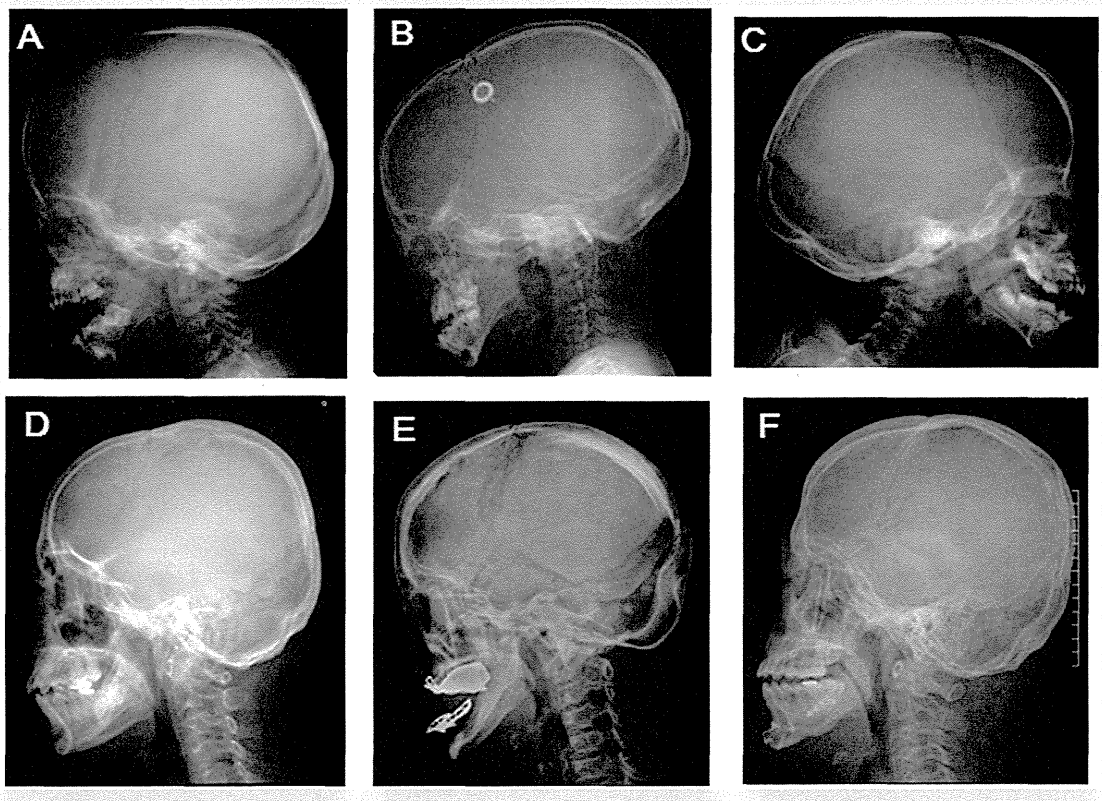

FIG. 2. Lateral skull radiographs. All patients showed Wormian bones. A: Patient 1 at 2 years and 11 months of age. B: Patient 2 at 13 years of age. C: Patient 3 at 2 years of age. D: Patient 4 at 31 years of age. E: Patient 5 at 41 years of age. F: Patient 6 at 20 years of age.

(Fig. 1F). Radiographs showed Wormian bone at the lambdoidal sutures (Fig. 2C) and acroosteolysis in the hands and feet (Fig. 4G,I), although osteoporosis and compression fractures were not noted (Fig. 3D). The bone mineral density of the lumbar spine was 0.873 g/cm^2 according to dual-energy X-ray absorptiometry, which corresponded to a T score of −2.0. The urine *N*-telopeptide of collagen type I, an osteoclast marker, was normal at 20.5 nmol BCE/mmolCr (normal values for premenopausal females = 9.3–54.3). The expression of the osteoblast marker serum bone-specific alkaline phosphatase (BAP) was also normal at 22.8 U/L. She did not display early loss of permanent teeth, pathological fractures, or any hearing or visual impairments.

Patient 5

Patient 5, a Korean woman, now 41 years of age has been described previously [Hwang et al., 2011]. She presented with mid-facial hypoplasia, micrognathia, short hands with pseudo-clubbing at the finger tip, malocclusion and loss of teeth, and patent ductus arteriosus. Her height was 139 cm (<3rd centile of Korean females). She had persistent pain in both hands and feet, and intermittent back pain. Radiographs showed Wormian bones with persistent patent cranial sutures, bathrocephaly (Fig. 2E), osteoporosis without compression fractures in the spine (Fig. 3E), and acroosteolysis in both hands and feet. The bone mineral density of her lumbar spine was 0.678 g/cm^2 according to dual-energy X-ray absorptiometry, which corresponded to T scores of −3.0.

Patient 6

Patient 6, a Korean man, now 20 years of age has been described previously [Han et al., 2010]. His developmental history was unremarkable. He presented with bushy eyebrows, mid-facial flattening with a wide nose, micrognathia, and distal clubbing fingers. At 19 years of age, his height was 168 cm (25th centile of Korean males). He underwent an operation for malocclusion of the teeth. He developed slow, progressive back pain and was found to have multiple spinal fractures and osteoporosis. Radiographs showed Wormian bones in the lambdoidal suture (Fig. 2F), osteoporosis with non-traumatic compression fractures throughout the lower thoracic and lumbar spine (Fig. 3F), and bilateral symmetrical acroosteolysis of the hands (Fig. 4I) and feet. The bone densitometry of the first lumbar vertebral body was

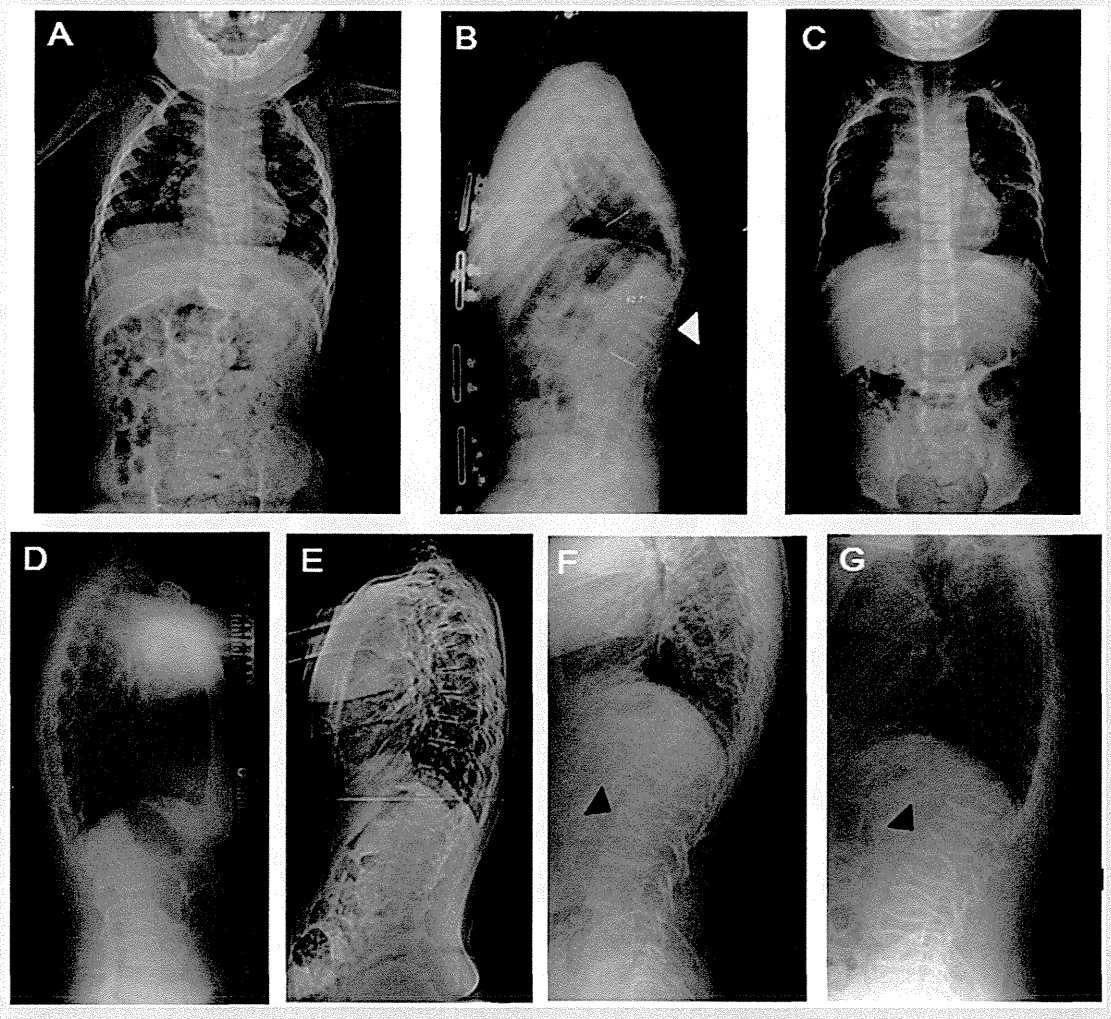

FIG. 3. Radiographs of the spine. A: Patient 1 at 2 years and 4 months of age. B: Patient 2 at 14 years of age. Osteoporosis with vertebral compression was indicated by white arrow heads. C: Patient 3 at 2 years of age. D: Patient 4 at 31 years of age. E: Patient 5 at 41 years of age. Patient 6 at 20 years of age (F) and his mother, Patient 7 at 46 years of age (G) showed biconcave shape of compression fractures [black arrow heads].

0.384 g/cm^2, corresponding to a T score of −6.1 and osteoporosis was evident.

Patient 7

Patient 7 is Korean woman, who is currently 46 years of age and is an affected mother of Patient 6. She was examined after her son was found to have an abnormality during mutation analysis. She shared similar facial features with her son. Her height was 150 cm (10th centile of Korean females). She experienced premature loss of the molar teeth and received implanted dentures at 40 years of age. She had longstanding back pain but received no further investigation. A skeletal survey detected Wormian bones in the lambdoidal suture, platybasia, marked compression fractures throughout the lumbar spine, and generalized osteoporosis (Fig. 3G). However, she did not present with acroosteolysis in her hands.

Mutation Analysis

After obtaining informed consent, genomic DNA was isolated from the peripheral leukocytes of the patients. Each exon and the flanking intronic sequences of *NOTCH2* were amplified using primers based on GenBank sequences (Supplementary eTable I—see Supporting Information online, GenBank accession number: NC_000001.10). The M13 reverse or forward sequence was added to the 5′ end of the polymerase chain reaction (PCR) primers and used as a sequencing primer. After purification, the PCR samples were directly sequenced using the ABI BigDye terminator Cycle Sequencing Kit (Applied Biosystems, Foster City, CA). Reactions were run

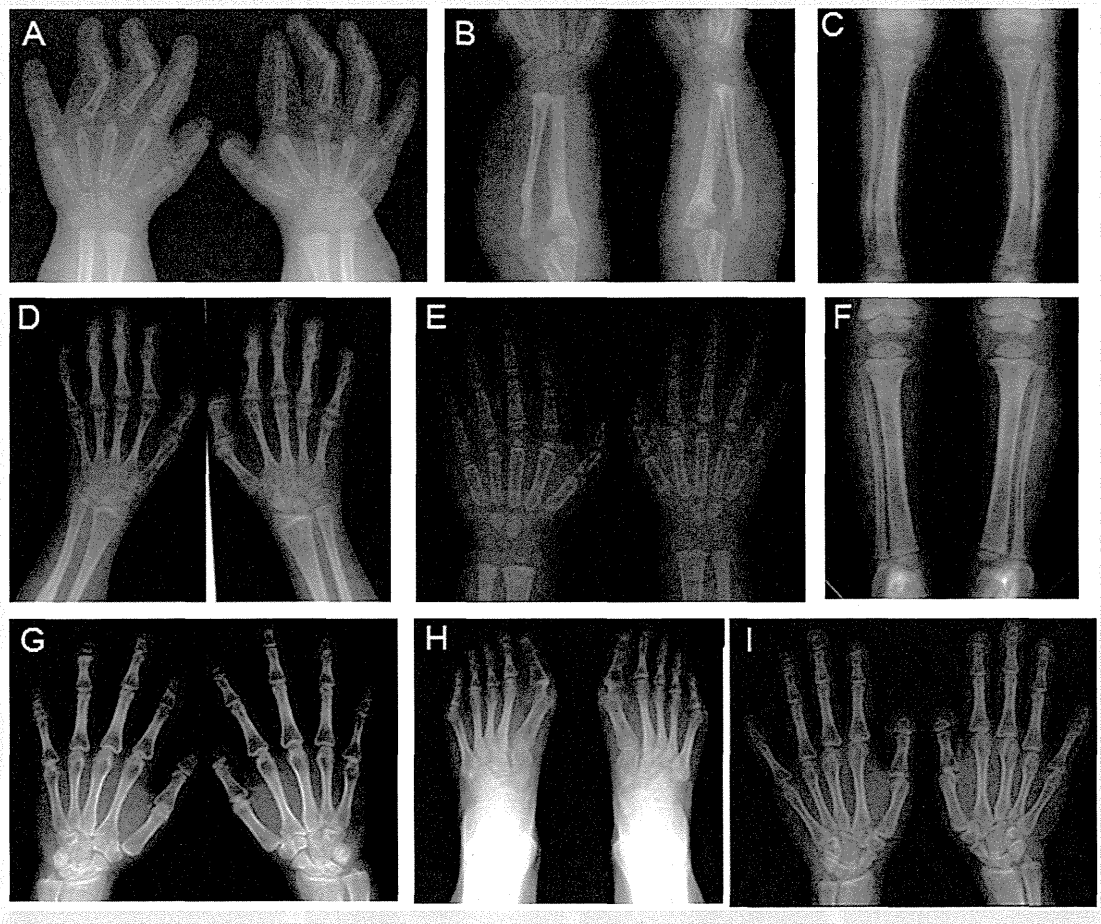

FIG. 4. Radiographs of the hands and feet. Patient 1 showed acroosteolysis of both the second and fifth fingers along with slender short tubular bones (A), twisted radii with proximal radioulnar dislocation (B), bowed tibiae and serpentine fibulae (C). Patient 2 at 14 years of age; acroosteolysis of the distal phalanges evident (D). Patient 3 at 2 years of age showing no acroosteolysis (E), and mild bowing tibiae (F). Bilaterally symmetrical acroosteolysis in distal phalanges was shown in Patient 4 (G/H) and Patient 6 (I).

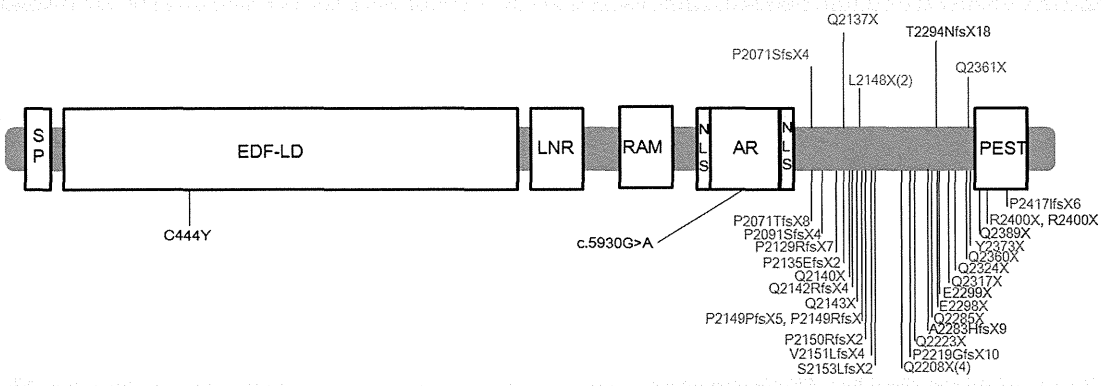

FIG. 5. Domain organization and identified *NOTCH2* mutations in HCS (red letter), SFPKS (blue letter), and Alagille syndrome (black letter). The mutations detected in this study are shown above the domain structure. The figures in parenthesis indicate the number of families. The functional domains are indicated as follows: SP, signal peptide; EDF-LD, EGF-like domain; LNR, Lin-Notch repeat; RAM, RAM 23 domain; NLS, nuclear localization signal; AR, Ankyrin repeats; PEST, proline-glutamic acid-serine-threonine-rich domain.

TABLE I. Characteristics of 34 Patients With NOTCH2 Mutations

	Patient 1	Patient 2	Patient 3	Patient 4	Patient 5	Patient 6	Patient 7	23 Patients with HCS and NOTCH2[a]	4 Patients with SFPKS and NOTCH2[b]	Total 34 patients with NOTCH2 (%)	Frequency in HCS[c] (%)
Gender	F	F	F	F	F	M	F				
Age	2	14	2	31	41	20	46				
Nucleotide	c.6883_6884ins A	c.7081C>T	c.6409G>T	c.6190_6212dup	c.6428T>C	c.6428T>C	c.6428T>C				
Protein	p.Thr2294AsnfsX18	p.Gln2361X	p.Glu2137X	p. Pro2071AsnfsX4	p.Leu2148X	p.Leu2148X	p.Leu2148X				
Inheritance	De novo	De novo	De novo	De novo	De novo	Familial	Familial				
Craniofacial Findings											
Synophrys	−	+	+	+	+	+	+	11/11	1/3	86 (18/21)	46
Midfacial flattening	+	+	+	+	+	+	+	1/3	0/3	62 (8/13)	32
Downslanted palpebral fissures	−	+	+	+	+	+	+	14/14	0/3	83 (20/24)	21
Hypertelorism	+	+	−	+	+	+	+	23/23	2/3	94 (31/33)	37
Wide nose	+	+	+	−	+	+	+	14/14	1/3	88 (21/24)	39
Long philtrum	+	+	+	−	+	+	+	23/23	3/4	94 (32/34)	40
Thin lips	+	+	+	+	+	+	+	2/2	2/3	92 (11/12)	n.d.
Low set ears	+	+	−	−	+	+	+	23/23	4/4	94 (32/34)	26
Retro/micrognathia	+	+	+	+	+	+	−	19/23	4/4	85 (29/34)	56
Coarse hair	+	+	−	+	+	+	+	1/1	n.d.	88 (7/8)	28
Coarse/dry skin	−	+	−	+	+	+	−	n.d.	1/1	75 (6/8)	7
Abnormal dentition	+	+	−	+	+	−	+	16/23	3/4	71 (24/34)	67
Hearing impairment	+	+	−	−	−	−	−	9/11	4/4	68 (15/22)	33
Congenital heart defect	+	+	+	−	+	−	−	3/23	4/4	32 (11/34)	12
Polycystic kidneys	+	−	−	−	−	−	−	4/22	3/4	24 (8/33)	14
Short stature	+	+	+	−	+	−	−	10/22	3/4	52 (17/33)	51
Developmental delay	+	+	−	−	−	−	−	0/12	1/4	13 (3/23)	18
Radiographic findings											
Acroosteolysis hands and feet	+	+	−	+	+	+	−	21/23	1/4	79 (27/34)	84
Womian bone	+	+	+	+	+	+	+	12/12	2/3	95 (21/22)	67
Platybasia/basilar impression	−	+	−	−	+	+	+	8/12	1/3	59 (13/22)	53
Osteoporosis	+	+	−	−	+	+	+	19/23	3/4	79 (27/34)	60
Fibular bowing	+	+	−	−	−	−	−	1/12	4/4	30 (7/23)	9
Spinal compression/ fracture	−	+	−	−	+	+	+	9/23	0/4	38 (13/34)	49
Fracture of long bones	+	+	−	−	−	−	−	0/3	1/4	21 (3/14)	28

[a]Marik et al. [2006], McKiernan [2007], Isidor et al. [2011a], Majewski et al. [2011].
[b]Majewski et al. [1993], Rosser et al. [1996], Albano et al. [2007], Gray et al. [2012], Isidor et al., [2011b].
[c]Brennan and Pauli [2001].

on an ABI 3100 semi-automated sequencing analyzer (Applied Biosystems). The DNA sequences were analyzed using FinchTV version 1.4.0 (Geospiza, Inc., Seattle, WA).

All patients had heterozygous, truncating mutations in exon 34 of *NOTCH2*. Patient 1 had c.6883_6884 ins A (p. Thr2294Asn fsX18), Patient 2 c.7081C>T (p.Gln2361X), Patient 3 c.6409 G>T (p. Glu2137X), and Patient 4 c.6190_6212dup (p.Pro2071AsnfsX4; Supplementary eFig. 1—see Supporting Information online). These mutations were previously unreported. Patients 5–7 had a recurrent mutation, c.6428T>C (p.Leu2148X).

DISCUSSION

In this study, we analyzed six HCS patients and one SFPKS patient with heterozygous mutations in *NOTCH2*. In previous reports on 48 patients from the 36 families, all patients had premature termination mutations in exon 34 (Fig. 5). All known HCS- or SFPKS-related *NOTCH2* mutations are dispersed throughout exon 34. Even the most common recurrent mutation (Gln2208X) was found only in four of the 36 families. In our series, we found Thr2294Asn fsX18 caused SFPKS, Gln2361X caused severe HCS with serpentine fibula, and Pro2071AsnfsX4 caused mild HCS. The patient with Glu2137X was too young to verify the final skeletal phenotype. It seems impossible to predict the clinical outcome from the mutation site.

Table I summarizes clinical and radiological manifestations in our series and all previously reported patients with *NOTCH2* mutations whose clinical manifestations are available (29 patients with HCS and five patients with SFPKS) [Majewski et al., 1993, 2011; Rosser et al., 1996; Marik et al., 2006; Albano et al., 2007; McKiernan, 2007; Isidor et al., 2011a,b; Gray et al., 2012]. We found 13 manifestations including synophrys, downslanted palpebral fissures, hypertelorism, wide nose, long philtrum, thin lips, low set ears, retro/micrognathia, coarse hair, coarse/dry skin, acroosteolysis, Wormian bones, and osteoporosis in >75% of *NOTCH2*-positive patients. Acroosteolysis is a characteristic clinical feature of HCS that usually develops during late childhood or adolescence [Brennan and Pauli, 2001]. Patient 7, 46 years of age, did not present acroosteolysis. However, acroosteolysis and osteoporosis with recurrent fractures were noted during infancy in Patient 1. In SFPKS patients, we observed the characteristic manifestations of HCS noted by Brennan et al. in their study including retro/micrognathia in five patients; abnormal dentition and short stature in four; Wormian bone in three; mid-facial flattening, coarse hair, and platybasia in one. In contrast, hearing impairment was observed in 10 HCS patients, polycystic kidneys in 4, and fibula bowing in 2. Serpentine fibula was observed in Patient 2, who developed unusually severe osteoporosis during adolescence. Thus, Patient 2 was considered to have an intermediate severity between HCS and SFPKS. These results suggest that truncating mutations in exon 34 of *NOTCH2* would cause a disorder, mainly characterized by abnormal bone turnover with various degrees of severity and occasionally accompanied by craniofacial features, cardiac, and renal defects.

In conclusion, clinical and molecular data in our series and previously reported patients suggest that HCS and SFPKS are a single disorder with variable degree of expression. This variability may be related to other modifier effects on possible truncating mutations in exon 34 of *NOTCH2*. Further analysis is needed to elucidate the pathogenesis of truncating mutation in exon 34 of *NOTCH2* on bone metabolism as well as various systems.

ACKNOWLEDGMENTS

The authors appreciate the patients and their families for their cooperation. We are also thankful to Tomomi Yamaguchi for her technical assistance.

REFERENCES

Albano LM, Bertola DR, Barba MF, Valente M, Robertson SP, Kim CA. 2007. Phenotypic overlap in Melnick-Needles, serpentine fibula-polycystic kidney and Hajdu-Cheney syndromes: A clinical and molecular study in three patients. Clin Dysmorphol 16:27–33.

Brennan AM, Pauli RM. 2001. Hajdu-Cheney syndrome: Evolution of phenotype and clinical problems. Am J Med Genet 100:292–310.

Currarino G. 2009. Hajdu-Cheney syndrome associated with serpentine fibulae and polycystic kidney disease. Pediatr Radiol 39:47–52.

Exner GU. 1988. Serpentine fibula-polycystic kidney syndrome. A variant of the Melnick-Needles syndrome or a distinct entity? Eur J Pediatr 147: 544–546.

Gray MJ, Kim CA, Bertola DR, Arantes PR, Stewart H, Simpson MA, Irving MD, Robertson SP. 2012. Serpentine fibula polycystic kidney syndrome is part of the phenotypic spectrum of Hajdu-Cheney syndrome. Eur J Hum Genet 20:122–124.

Han EJ, Mun JI, An SY, Jung YJ, Kim OH, Chung YS. 2010. A case report of Hajdu-Cheney syndrome. Endocrinol Metab 25:152–156[Korean].

Hwang S, Shin DY, Moon SH, Lee EJ, Lim SK, Kim OH, Rhee Y. 2011. Effect of zoledronic acid on acro-osteolysis and osteoporosis in a patient with Hajdu-Cheney syndrome. Yonsei Med J 52:543–546.

Isidor B, Lindenbaum P, Pichon O, Bézieau S, Dina C, Jacquemont S, Martin-Coignard D, Thauvin-Robinet C, Le Merrer M, Mandel JL, David A, Faivre L, Cormier-Daire V, Redon R, Le Caignec C. 2011. Truncating mutations in the last exon of *NOTCH2* cause a rare skeletal disorder with osteoporosis. Nat Genet 43:306–308.

Isidor B, Le Merrer M, Exner GU, Pichon O, Thierry G, Guiochon-Mantel A, David A, Cormier-Daire V, Le Caignec C. 2011. Serpentine fibula-polycystic kidney syndrome caused by truncating mutations in *NOTCH2*. Hum Mutat 32:1239–1242.

Kaplan P, Ramos FJ, Zackai EH, Bellah RD, Kaplan BS. 1995. Cystic kidney disease in Hajdu-Cheney syndrome. Am J Med Genet 56:25–30.

Majewski F, Enders H, Ranke MB, Voit T. 1993. Serpentine fibula-polycystic kidney syndrome and Melnick-Needles syndrome are different disorders. Eur J Pediatr 152:916–921.

Majewski J, Schwartzentruber JA, Caqueret A, Patry L, Marcadier J, Fryns JP, Boycott KM, Ste-Marie LG, McKiernan FE, Marik I, Van Esch H, FORGE Canada Consortium, Michaud JL, Samuels ME. 2011. Mutations in *NOTCH2* in families with Hajdu-Cheney syndrome. Hum Mutat 32:1114–1117.

Marik I, Kuklik M, Zemkowa D, Kozlowski K. 2006. Hajdu-Cheney syndrome: Report of a family and a short literature review. Sustralas Radiol 50:534–538.

McKiernan FE. 2007. Integrated anti-remodeling and anabolic therapy for the osteoporosis of Hjdu-Cheney syndrome. Osteoporos Int 18:245–249.

Ramos FJ, Kaplan BS, Bellah RD, Zackai EH, Kaplan P. 1998. Further evidence that the Hajdu-Cheney syndrome and the "serpentine

fibula-polycystic kidney syndrome" are a single entity. Am J Med Genet 78:474–481.

Rosser EM, Mann NP, Hall CM, Winter RM. 1996. Serpentine fibula syndrome: Expansion of the phenotype with three affected siblings. Clin Dysmorphol 5:207–212.

Simpson MA, Irving MD, Asilmaz E, Gray MJ, Dafou D, Elmslie FV, Mansour S, Holder SE, Brain CE, Burton BK, Kim KH, Pauli RM, Aftimos S, Stewart H, Kim CA, Holder-Espinasse M, Robertson SP, Drake WM, Trembath RC. 2011. Mutations in *NOTCH2* cause Hajdu-Cheney syndrome, a disorder of severe and progressive bone loss. Nat Genet 43:303–305.

Takatani R, Someya T, Kazukawa I, Nishimura G, Minagawa M, Kohno Y. 2009. Hajdu-Cheney syndrome: Infantile onset of hydrocephalus and serpentine fibulae. Pediatr Int 51:831–833.

Zanotti S, Canalis E. 2012. Notch regulation of bone development and remodeling and related skeletal disorders. Calcif Tissue Int 90:69–75.

Expanded newborn mass screening with MS/MS and medium-chain acyl-CoA dehydrogenase (MCAD) deficiency in Japan

Seiji Yamaguchi[1], Jamiyan Purevusren[1], Hironori Kobayashi[1], Yuki Hasegawa[1], Yuichi Mushimoto[1], Kenji Yamada[1], Tomoo Takahashi[1], Midori Furui[1], Takeshi Taketani[1], Seiji Fukuda[1], Toshiyuki Fukao[2], Yosuke Shigematsu[3]

1) Department of Pediatrics, Shimane University, Japan
2) Department of Pediatrics, Gifu University, Japan
3) Department of Medical Science and Pediatrics, Fukui University, Japan

Abstract

Expanded newborn mass screening (NBS) with tandem mass spectrometry (MS/MS) and medium-chain acyl-CoA dehydrogenase (MCAD) deficiency in Japan are described. Prognosis of patients with inborn metabolic disease was compared between groups detected in the symptomatic and pre-symptomatic stages. Furthermore, clinical, biochemical and genetic findings of Japanese children with MCAD deficiency, which is a most important target of MS/MS screening, was investigated. Our study concluded as follows: 1) the detection incidence in MS/MS screening in Japan is totally about 1 in 9,000, which might be smaller than that of the other countries; 2) Outcomes of patients detected by NBS (pre-symptomatic stage) is more favorable than that of cases detected after symptomatic onset; 3) the incidence of MCAD deficiency in the Japanese population is 1 in 110 thousands, which is approximately 10 times smaller than that in Caucasian; 4) Japanese patients with MCAD deficiency have a common mutation, c.449-452delCTGA, which covers about 45% of alleles of MCAD gene, but not have 985A>G, which is a common mutation of Caucasians patients; 5) genotype/phenotype correlation was not observed in MCAD deficiency; 6) prognosis of the non-symptomatic group is much more favorable than that of the symptomatic group. In conclusion, it is indicated that detection of inborn metabolic disease in the pre-symptomatic stage by NBS is essential to prevent children affected with target diseases of NBS including MCAD deficiency from neurological impairments or infant death.

Key words

expanded newborn mass screening, MS/MS, MCAD deficiency, genotype/phenotype correlation, prevention of neurological impairment

<Correspondence>
Seiji YAMAGUCHI, MD
Professor, Department of Pediatrics,
Shimane University School of Medicine
89-1, En-ya-cho, Izumo, Shimane 693-8501, Japan
Tel:+81-853-20-2220 Fax:+81-853-20-2215
E-mail:seijiyam@med.shimane-u.ac.jp

1. Introduction

The expanded newborn screening (NBS) using tandem mass spectrometry (MS/MS) is becoming popular worldwide. In Japan, a pilot screening was initiated at Fukui University in 1997 (1), and the national

project of MS/MS screening (Principle Investigator, Dr. Seiji Yamaguchi, Shimane University) funded by Grant-in-Aid for Scientific Research from the Ministry of Health, Labour, and Welfare was started in 2004. For the pilot screening, about 10 laboratories in Japan joined up to 2012. The Japanese government issued notice urging implementation of MS/MS to NBS in 2011. Eventually, the MS/MS screening is becoming spread from 2012 to 2013 (2), and will initiate officially nationwide in next year (2014).

In the expanded NBS, it is considered that medium-chain acyl-CoA dehydrogenase (MCAD) deficiency is a most important screening target, particularly in Caucasian people, because the incidence is high (1 in 10,000), and MCAD deficiency is a causative disease of sudden infant death, and preventable by detection in NBS (3). In this paper, clinical and genetic aspects of MCAD deficiency as well as the results of the pilot MS/MS screening in Japan are described.

2. Pilot MS/MS Screening In Japan

a) Results of pilot MS/MS screening in Japan

A total number of babies screened by MS/MS during the period between 1997 and 2012 was 1,949,987 (about 1.95 million), and 217 cases affected with disease were found as shown in Table 1. The detection incidence of Japanese babies was calculated to be 1 in 8,986, while that in USA was estimated to be 1 in 4,353 (4). The prevalence of Japanese is likely smaller than that of the other countries.

b) The detection prevalence of each disease group

The incidence of amino acidemias was totally 1 in 27 thousands; that of organic acid disorders, 1 in 22 thousands; and that of fatty acid disorders, 1 in 34 thousands. The most common disease in Japan was propionic acidemia, which was found in 1 in 45,349 (about 45 thousands); and phenylketonuria, 1 in 52,702 (53 thousands); followed by methylmalonic acidemia and MCAD deficiency, each of which in 1 in 108,333 (110 thousands). A considerable number of Japanese patients with propionic acidemia show a mild phenotype with a common mutation, 1304T>C (Y435C) in *PCCB* gene (5).

c) Comparison of outcomes between cases detected by NBS and by tests after symptomatic onset

Outcomes of cases with organic and fatty acid disorders detected in NBS were compared with those detected after symptomatic onset by MS/MS, GC/MS and/or molecular investigation in Shimane University. As shown in Table 2, in organic acid disorder, normal development was achieved in 58 of 70 cases (83%) of the NBS group, as of at least 1 year of age. In contrast, normal development was gotten in only 28 of 114 cases (19%) in the "symptomatic" group.

In fatty acid disorder, normal development was achieved in 40 of 45 cases (89%) in the NBS group, although that was in 25 of 52 cases (48%) in the symptomatic group. Hence, beneficial effect of NBS using MS/MS was indicated. Through the results of the pilot study, we proposed 16 kinds of disease which should be screened as primary targets as marked with black circle in Table 1, in consideration of the false negative rate, complexity of diagnostic approaches, or the benefit of detection by NBS.

Table 1. Results of the pilot screening using MS/MS in Japan (1997 to 2012)

Disease		No. of Cases	Incidence (Japan)	Estimated in USA*
AMINO ACIDEMIA		72	(1:27 K)	(1:15 K)
• Phenylketonuria		37	1: 53 K	1: 19 K
• MSUD		1	1: 1,950 K	1: 159 K
• Homocystinuria		3	1: 650 K	1: 38 K
• Citrulinemia type I		6	1: 330 K	1: 173 K
• Argininosuccinic A		2	1: 980 K	1: 591 K
Citrin deficiency		23	1: 85 K	n.a.
ORGANIC ACIDEMIA		87	(1: 22 K)	(1:16 K)
• Methylmalonic acidemia		18	1: 110 K	1: 67 K
• Propionic acidemia		43	1: 45 K	1: 276 K
• Isovaleric acidemia		3	1: 650 K	1: 129 K
• MCD		3	1: 650 K	1: 1,380K
• Methylcrotonylglycinuria		13	1: 150 K	1: 44 K
• HMGL deficiency		—	—	1: 1,380K
• Glutaric acidemia type1		7	1: 280 K	1: 109 K
β-ketothiolase deficiency		—	—	1: 591 K
FATTY ACID DISORDER		58	(1: 34 K)	(1:10 K)
• CPT1 deficiency		5	1: 390 K	n.a.
• VLCAD deficiency		12	1: 160 K	1: 69 K
• MCAD deficiency		18	1: 110 K	1: 17 K
• TFP/LCHAD deficiency		2	1: 980 K	1: 276 K
CPT2 deficiency		7	1: 280 K	n.a.
CACT deficiency		—	—	n.a.
Glutaric acidemia type 2		6	1: 330 K	n.a.
Carnitine uptake defect		7	1: 280 K	1: 49 K
SCHAD deficiency		1	1: 1,950 K	n.a.
TOTAL	Affected cases	217	1: 8,986	1: 4,353
	Screened babies	1,949,987		

•, primary target disease in the MS/MS screening in Japan. "K" means thousands. * Estimated incidence in USA, based on live birth for 2006 (n=4,138,349) (4). Abbreviation: −, not detected; n.a., not applicable; MCD, multiple carboxylase deficiency; HMGL, 3-hydroxy-3- methyl-glutaryl-CoA lyase; CPT1 and CTP2, carnitine palmitoyl transferase-I and -II, respectively; VLCAD and MCAD, very-long-, and medium-chain acyl-CoA dehydrogenase, respectively; TFP, mitochondrial trifunctional protein; CACT, carnitine acylcarnitine translocase; LCHAD and SCHAD, long- and short-chain 3-hydroxyacyl-CoA dehydrogenase, respectively.

3. Clinical, Biochemical and Genetic Investigation of Japanese MCAD Deficiency

a) Outline of MCAD deficiency

MCAD deficiency was first discovered in children with sudden infant death syndrome-like illness in 1982, and has been found at an incidence of 1 in 10,000. A common mutation, 985A>G, covering about 90% of the alleles in this disease was seen among Caucasian population. Acute symptoms of MCAD deficiency include acute

Table 2. Comparison of outcomes between presymptomatic and symptomatic detection cases in Japanese children with organic academia and fatty acid disorder.

Disease	NBS (MS/MS screening)	Symptomatic (Shimane)
No. of cases	115	196
ORGANIC ACID DISORDER	70	144
Normal development	58 (83%)	28 (19%)
Handicaps or death	12 (17%)	116 (81%)
FATTY ACID DISORDER	45	52
Normal devlopment	40 (89%)	25 (48%)
Handicaps or death	5 (11%)	27 (52%)

NBS, newborn mass screening, MS/MS screening, cases detected by the pilot study between 2004 and 2011. Symptomatic, cases after symptomatic onset and detected by MS/MS, GC/MS or molecular tests in Shimane University from 2001 to 2011.

encephalopathy-like symptoms, or even sudden death (6), following after long fasting or infection, although the patients have no symptoms in the stable condition. Concerning the prognosis, it has been claimed that as many as 35% of MCAD deficiency patients are asymptomatic lifelong, but that over 25% of the symptomatic cases die suddenly during the first episodic attack (3).

Abnormal laboratory tests in the acute condition include hypoglycemia or hyperammonemia. Biochemical markers in MS/MS analysis of blood acylcarnitines are elevation of C8, C6 or C10, or C8/C10. Elevation of hexanoylglycine (HG) and suberylglycine (SG) as well as dicarboxylic acids is often observed by GC/MS analysis of urinary organic acids.

b) Prevalence of MCAD deficiency in Japan

According to the results of pilot screening using MS/MS, MCAD deficiency was found at the incidence of 1 in 110 thousands, and was most common among fatty acid disorders in the pilot study of Japan, as shown in Table 1. However, the incidence is about 10 times smaller than that of Caucasian whose incidence is 1 in 10 thousands (3).

c) Subjects of MCAD deficiency

Ages at onset, and diagnosis, clinical, biochemical and genetic findings of a total 20 Japanese cases whose blood C8 acylcarnitine, a diagnostic marker of MCAD deficiency, was over the cut off value (0.3 nmol/mL) in MS/MS analysis were investigated (Table 3). Cases 1 through 9 were identified after symptomatic onset (symptomatic group), while cases 10 through 18 were detected in the non-symptomatic or pre-symptomatic stage (non-symptomatic group). Cases 10 through 17 were detected by NBS while Case 18 was by the sibling screening using MS/MS. Acylcarnitine analysis was performed at Shimane University or the other laboratories. GC/MS analysis (7) and gene analysis (8) were performed at Shimane University. The final diagnosis was confirmed by gene analysis, which revealed that cases 19 and 20 were heterozygotes (carrier group). Clinical information was surveyed using questionnaire.

Table 3. Clinical, biochemical and genetic profiles of Japanese cases of MCAD deficiency

No.	Age at onset	Age at diag.	NBS	MS/MS	GC/MS		Genotype		Outcome
				C8 (<0.3)	HG	SG	Allele 1	Allele 2	
Symtpomatic group									
1	8m	8m	−	5.97	11.1	44.5	c.449-452del	c.157C>T	impair
2	1y0m	1y0m	−	4.52	n.a	n.a	IVS4+1G>A	c.422 A>T	SID
3[a]	1y0m	8y10m	−	1.57	45.4	29.6	c.449-452del	c.449-452del	impair
4	1y1m	1y1m	−	7.00	14.7	112.2	del. ex 11-12	del. ex 11-12	impair
5	1y3m	1y3m	−	high*	n.a	n.a	del. ex 11-12	del. ex 11-12	impair
6[b]	1y4m	1y4m	−	3.33	9.9	15.3	c.449-452del	c.449-452del	impair
7	1y7m	1y7m	−	4.12	6.1	6.4	c.275C>T	c.157C>T	impair
8[a]	1y8m	1y8m	−	4.75	69.3	1.2	c.449-452del	c.449-452del	SID
9	2y2m	2y2m	−	1.71	n.a	n.a	c.449-452del	c.449-452del	normal
Non-symptomatic group									
10	−	5d	+	5.92	12.9	14.8	c.1085G>A	c.843A>T	normal
11	−	5d	+	5.37	6.3	39.9	c.449-452del	c.154A>G	normal
12	−	5d	+	4.82	15.3	3.8	IVS3+2T>C	c.843 A>T	normal
13	−	5d	+	4.04	n.a	n.a	c.449-452del	c.212 G>A	normal
14	−	5d	+	2.78	11.5	5.9	c.449-452del	c.134 A>G	normal
15	−	5d	+	2.59	3.1	(-)	c.1085G>A	c.1184A>G	normal
16	−	5d	+	2.58	(-)	3.2	c.449-452del	IVS3+5G>A	normal
17	−	5d	+	0.49	9.7	1.5	c.449-452del	c.820 A>C	normal
18[b]	−	5y5m	−	1.37	n.a	n.a	c.449-452del	c.449-452del	normal
Carrier group									
19	−	5d	+	0.44	(-)	(-)	c.845C>T	(-)	normal
20	−	4m	−	0.51	(-)	(-)	c.843A>T	(-)	normal

Cases 3 and 8 (a-a), and cases 6 and 18 (b-b) are sibling cases, respectively. Abbreviation: diag, diagnosis; NBS, newborn mass screening; −, none; +, NBS received; MS/MS, blood acylcarnitine analysis; GC/MS, urinary organic acid analysis; HG and SG, hexanoylglycine and suberylglycine, respectively; high*, elevated but detailed value not available. n.a, data not available in Shimane University; (-), not detected; SID, sudden infant death; c.449-452del, 4 base deletion of CTGA. impair, neurological impairments as sequallae. Unit: C8, nmol/mL (cut off, <0.3); HG and SG, peak area ratio to IS (%) (7) on GC/MS (normal, both undetectable).

d) Comparison between Symptomatic and non-symptomatic groups of MCAD deficiency

1) Ages at onset and diagnosis: In the symptomatic group, the ages at onset was 8 mo to 2 yr 2 mo. Cases 3 and 8, and cases 6 and 18, were siblings. In 9 cases of the non-symptomatic group, 8 cases were detected on 5 day after birth by NBS, and the other one (case 18) was identified at the age of 5 yr 5 mo by sibling screening.

2) Clinical findings of symptomatic case: In the symptomatic group, all 9 cases had acute encephalopathy- or sudden death-like illness in the acute stage. Hypoglycemia was observed in all 7 cases tested, while hyperammonemia was seen in 4 of the 9 cases.

3) Biochemical findings: As shown in Table 2, C8 (cut off, <0.3 nmol/mL) ranged between 1.57 and 7.00 in the symptomatic group, while C8 did between 0.49 and 5.92

in the non-symptomatic group. No significant difference between these two groups was seen in the level of C8. The C8 value of the carrier group (cases 19 and 20) was 0.44 and 0.51, respectively, which was lower compared to those of the 18 affected cases. No significant difference was seen in the urinary excretion amounts of HG or SG between these two groups (Table 3).

4) Gene mutation: c.449-452delCTGA (c.449del4) was identified in 16 of 36 alleles (44%) in 18 Japanese patients with MCAD deficiency. The homozygote of c.449del4 mutants were observed in 4 and 1 cases in the symptomatic and non-symptomatic groups, respectively. A common mutation, 985A>G, found in Caucasian population was never identified in Japanese cases (8). On the other hand, it was reported that the c.449del4 mutation was in 3 of 5 alleles of 3 Korean MCAD deficiency cases (9). It would be interesting to investigate and compare the genotypes of Japanese MCAD deficiency with those of the other Asian countries and the other ethnic groups.

5) Outcomes: With respect to the outcomes, 8 of 9 cases of the symptomatic group resulted in severe handicaps or sudden death, whereas all 9 cases of the non-symptomatic group showed normal development and growth (Table 3). It was likely that there were no genotype/phenotype correlation, although existence of the correlation is not clear enough in the present point (10). These findings indicate that pre-symptomatic detection is important for the favorable outcome in MCAD deficiency. Namely, NBS is essential (11, 12). Furthermore, our data suggests no clear genotype/phenotype in MCAD deficiency.

4. Conclusion

Our study indicated that: 1) the detection incidence in MS/MS screening is totally about 1 in 9,000 in Japan, which might be 2 times smaller than that of other countries; 2) the outcomes of patients detected by NBS is more favorable compared with that of cases detected after symptomatic onset; 3) the incidence of MCAD deficiency is 1 in 110 thousands in Japanese population. This is approximately 10 times smaller than that in Caucasian population; 4) 45% of alleles of *MCAD* gene in Japanese patients have a common mutation, c.449-452delCTGA. The genetic background of Japanese cases is likely the same with Korean patients, but different from those in Caucasians with MCAD; 5) clinical severity of MCAD deficiency may be similar despite the different genetic mutations, suggesting that genotype does not necessarily predict phenotype in MCAD deficiency; 6) prognosis of the symptomatic cases with MCAD deficiency was poor, whereas that of the non-symptomatic group was excellent, indicating "pre-symptomatic detection" is essential to prevent children affected with MCAD deficiency from impairments or sudden death.

Acknowledgement

This study was supported in part by Grants from the Ministry of Health, Labor and Welfare of Japan, and the Grants-in-Aid Scientific Research. We thank the group member of the National Promotion Project for Newborn Mass Screening (PI, S. Yamaguchi) for providing precious information of the patients.

References

1) Shigematsu Y, Hirano S, Hata I,

Tanaka Y, Sudo M, Sakura N, Tajima T, Yamaguchi S: Newborn mass screening and selective screening using electrospray tandem mass spectrometry in Japan, J Chromatogr B Analyt Technol Biomed Life Sci 77639-48, 2002.

2) Yamaguchi S: Annual report of the national project of the Neonatal Mass Screening funded by the Ministry of Health, Labor, and Welfare, Japan, 2013 (in Japanese).

3) Stanley CA, Bennet MJ: Disorders of mitochondrial fatty acid oxidation. Nelson's Texbook 19th ed. (eds by Berman RE, Kliegman RM, Jenson HB), Saunders, Philladelphia, p456-462, 2011.

4) Therrell B, Lorey F, Frazier D, Hoffman G, Boyle C, Green D, Devine O, Hannon H: Impact of Expanded newborn screening - United States, 2006. MMWR 57: 1012-1015, 2008.

5) Yorifuji T, Kawai M, Muroi J, Mamada M, Kurokawa K, Shigematsu Y, Hirano S, Sakura N, Yoshida I, Kuhara T, Endo F, Mitsubuchi H, Nakahata T: Unexpectedly high prevalence of the mild form of propionic acidemia in Japan: presence of a common mutation and possible clinical implications. Human Genet 111: 161-5, 2002.

6) Ding JH, Roe CR, Iafolla AK, Chen YT, Medium-chain acyl-coenzyme A dehydrogenase deficiency and sudden infant death, N Engl J Med 325: 61-62, 1991.

7) Kimura M, Yamamoto T, Yamaguchi S, Automated metabolic profiling and interpretation of GC/MS data for organic acidemia screening: a personal computer-based system, Tohoku J Exp Med 188: 317-334, 1999.

8) Purevsuren J, Hasegawa Y, Fukuda S, Kobayashi H, Mushimoto Y, Yamada K, Takahashi T, Yamaguchi S: Clinical and Molecular Aspects of Japanese Children with Medium Chain Acyl-CoA Dehydrogenase Deficiency. Mol Gen Met 107: 237-240. 2012.

9) Ensenauer R, Winters JL, Parton PA, Kronn DF, Kim JW, Matern D, Rinaldo P, Hahn SH: Genotypic differences of MCAD deficiency in the Asian population: novel genotype and clinical symptoms preceding newborn screening notification. Genet Med 7: 339-43, 2005.

10) Waddell L, Wiley V, Carpenter K, Bennetts B, Angel L, Andresen BS, Wilcken B: Medium-chain acyl-CoA dehydrogenase deficiency: genotype-biochemical phenotype correlations, Mol Genet Metab 87: 32-39, 2006.

11) Derks TG, Reijngoud DJ, Waterham HR, Gerver WJ, van den Berg MP, Sauer PJ, Smit GP: The natural history of medium-chain acyl CoA dehydrogenase deficiency in the Netherlands: clinical presentation and outcome,. J Pediatr 148: 665-670, 2006.

12) Wilcken B, Wiley V, Hammond J, Carpenter K: Screening newborns for inborn errors of metabolism by tandem mass spectrometry, N Engl J Med 348: 2304-2312, 2003.

受付日：平成25年11月12日

Effect of Topical Tafluprost on Optic Nerve Head Blood Flow in Patients With Myopic Disc Type

Satoru Tsuda, MD, Yu Yokoyama, MD, Naoki Chiba, MD, Naoko Aizawa, MD, Yukihiro Shiga, MD, Masayuki Yasuda, MD, Shunji Yokokura, PhD, MD, Takaaki Otomo, MD, Nobuo Fuse, PhD, MD, and Toru Nakazawa, PhD, MD

Purpose: To investigate the effect of topical tafluprost on optic disc blood flow in patients with myopic disc.

Materials and Methods: Forty-eight eyes in 24 patients with a myopic disc type (oval shaped) optic disc tilted to the temporal, with a crescent peripapillary atrophy were included in this study. Twenty-eight eyes were diagnosed as normal tension glaucoma and 20 eyes were in normal subjects. None had any treatment for glaucoma. Average age was 45.3 ± 11.9 years. One eye was treated with topical tafluprost and the fellow eye served as the control. Ocular blood flow was measured by laser speckle flowgraphy (LSFG-NAVI) at 30, 60, 90, and 120 minutes after tafluprost administration, and the mean blur rate (MBR) on the optic disc was analyzed. Blood pressure and intraocular pressure (IOP) were recorded.

Results: In all subjects, topical tafluprost (a) significantly reduced IOP versus baseline from 60 minutes after treatment (baseline: 15.2 ± 3.4 mm Hg, 60 min: 13.3 ± 3.2 mm Hg, $P = 0.001$, 90 min: 13.3 ± 3.6 mm Hg, $P = 0.002$, 120 min: 13.7 ± 3.4 mm Hg, $P = 0.007$); and (b) significantly increased the MBR versus baseline (60 min: + 4.3 ± 6.6%, $P = 0.008$, 90 min: + 5.0 ± 4.9%, $P < 0.001$, 120 min: + 6.7 ± 7.0%, $P < 0.001$).

Conclusions: Topical tafluprost increased MBR in the optic nerve head and significantly reduced IOP, effects that may represent beneficial treatment for glaucoma patients with a myopic disc type.

Key Words: blood flow, prostaglandin F2-α, normal tension glaucoma, myopia

(*J Glaucoma* 2013;22:398–403)

Ocular blood flow is thought to be a risk factor in the pathology of glaucoma, alongside intraocular pressure (IOP),[1–4] and a compromised local ocular blood flow may lead to visual-field deterioration. Since fluorescein angiography has revealed a filling defect in the optic nerve head (ONH) in patients with glaucoma,[5–9] an induced improvement in ocular blood flow may be an effective form of glaucoma treatment.

In our recent publication, 20% of the patients with glaucoma exhibited a decreased best corrected visual acuity (BCVA: < 20/20) due to glaucoma[10] and those patients with a severe by decreased BCVA (< 0.3) had a myopic disc type.[10] Furthermore, our hospital-based retrospective study on the advanced stage of normal tension glaucoma (NTG) revealed that a significant number of severe NTG patients had the myopic disc type.[11] When our fluorescein angiography study detected a filling defect in the temporal area of the tilted myopic disc,[10] we were motivated to investigate the ocular circulation, especially in glaucoma patients with a myopic disc type.

Ocular blood flow may be measured using the Heidelberg Retina Flowmeter,[12] color Doppler imaging,[13] laser speckle flowgraphy (LSFG),[14–17] or laser Doppler velocimetry.[18] LSFG, a noninvasive technique that can measure relative ONH blood flow using the laser speckle phenomenon,[15] is often employed to investigate the effect of glaucoma eye drops on the ocular circulation.[19] Recently, LSFG-NAVI, a newer version of LSFG, became commercially available, and in this machine the focusing of the acquired image is significantly improved. The intrasession reproducibility of mean blur rate (MBR) in ONH was excellent (coefficient of variation, 3.4 ± 2.0%).[20]

In Asia, the major type of glaucoma is NTG, not high-pressure glaucoma,[21] and there is a limitation to the lowering of IOP in patients with NTG.[22] A recently, excellent review on ocular blood flow suggested that a decreased ocular circulation is related to the prevalence and progression of glaucoma.[23] However, there is no published evidence that treatment aimed at restoring the ocular circulation can impede the progression of glaucoma, despite several studies investigating the increases in ONH blood flow achieved with clinically used topical antiglaucoma eye drops.[19,24,25] Tafluprost represents a new generation of potent FP-receptor agonists[26] and 2 recent studies of the effect of tafluprost instillation on ONH blood flow have reported vascular dilation during endothelin-1-induced arterial vessel constriction in an ex vivo rabbit experiment[27] and in monkeys in vivo.[28] We hypothesized that topical tafluprost might not only lower IOP, but also improve the ocular circulation in patients with NTG.

Therefore, in this study we investigated the effect of topical tafluprost on ONH blood flow using LSFG-NAVI both in glaucoma patients and in normal volunteers with the myopic disc type. We instilled topical tafluprost into only 1 eye, the fellow eye serving as control, and we compared the ocular blood flow in the ONH with the baseline value every 30 minutes until 120 minutes after the instillation.

MATERIALS AND METHODS

Eligibility of Participants

Forty-eight eyes in 24 participants with a myopic disc type (oval shaped) optic disc tilted to the temporal, with a

Received for publication February 23, 2011; accepted September 12, 2011.
From the Department of Ophthalmology, Tohoku University Graduate School of Medicine, Aoba-ku, Sendai, Miyagi, Japan.
Disclosure: The authors declare no conflict of interest.
Reprints: Toru Nakazawa, PhD, MD, Department of Ophthalmology, Tohoku University Graduate School of Medicine, 1-1 Seiryo-machi, Aoba-ku, Sendai, Miyagi 980-8574, Japan (e-mail: ntoru@oph.med.tohoku.ac.jp).

DOI:10.1097/IJG.0b013e318237c8b3

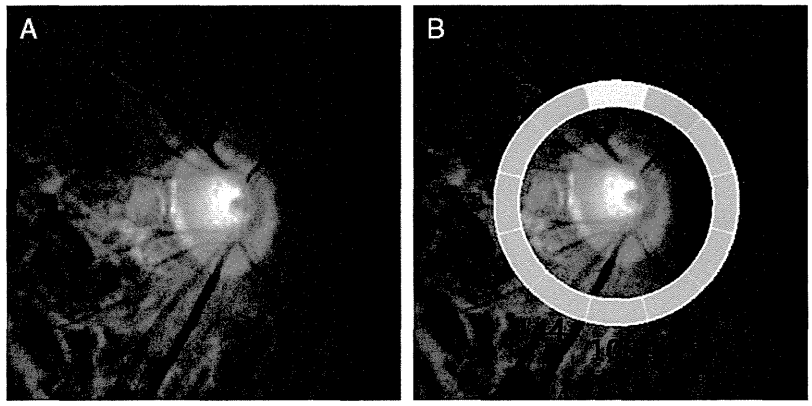

FIGURE 1. A, The fundus photograph shows a typical myopia-type optic disc. The optic disc is oval, is tilted to temporal side with crescent peripapillary atrophy. B, The colored circle and thickness (μm) on the fundus photograph showed retinal nerve fiber layer thickness. This patient had thin retinal nerve fiber layer in the 12 o'clock position.

crescent peripapillary atrophy were included in this study (Fig. 1A). The optic disc shape and condition was determined by the fundus photograph and retinal nerve fiber layer thickness around a optic disc obtained using 3-dimensional OCT-1000 (Topcon Corporation, Tokyo, Japan) (Fig. 1B). The participating group comprised of 28 eyes belonging to 14 glaucoma patients (age 52.3 ± 9.7; 37 to 70 y; male/female: 7/7) and 20 eyes in 10 healthy volunteers (age 35.5 ± 6.6; 25 to 42 y; male/female: 9/1). The glaucoma patients were under observation at our department of ophthalmology, and gave written informed consent to their participation in this study. This study followed the Tenets of the Declaration of Helsinki, and the institutional review board of Tohoku University approved the consent forms for this study. None of the 24 participants had previously had any antiglaucoma eye drops instilled, nor were any of them on any systemic medications that could alter the ocular blood flow, such as Ca^{2+}-channel blockers or β-blockers. Participants were excluded if: ocular diseases other than open-angle glaucoma were present, systemic diseases affecting the visual fields were present, they had undergone intraocular surgery, or their spherical equivalent was < -8 D. BCVA was measured using a standard Japanese decimal visual acuity chart, and the values were converted to logMAR units. IOP was measured by Goldmann applanation tonometry.

Administration of Topical Tafluprost

Tafluprost (TAPROS; Santen Pharmaceutical, Osaka, Japan) is a selective FP agonist with an IOP-lowering effect. It was recently reported that tafluprost improved the microcirculation in the healthy human ONH.[29] In each subject, 1 drop of 0.0015% tafluprost was instilled once into the eye that had the higher IOP or in which visual-field loss was more advanced. The fellow eye served as control. If the pupils of a given participant were too small to allow measurement of blood flow using LSFG-NAVI, 0.4% tropicamide (Mydrin M; Santen Pharmaceutical) was instilled into both the eyes. The IOP, ONH blood flow, blood pressure, and pulse rate were measured before treatment (0), and at 30, 60, 90, and 120 minutes after instillation of tafluprost. For those measurements, we used Goldmann applanation and an automated sphygmomanometer. Mean blood pressure was calculated from the blood pressure values, and ocular perfusion pressure (OPP) was calculated using the formula OPP = 2/3 mean blood pressure − IOP.

Diagnosis of Glaucoma

Glaucoma was diagnosed by the cupping of the optic disc and the corresponding visual-field loss. Automated perimetry was performed using a Humphrey Field Analyzer (SITA standard program 30-2). Reliability criteria included fixation losses, and false-positive and false-negative rates of $< 20\%$. Twenty-eight eyes had glaucomatous visual-field loss according to the Anderson-Pattela classification, as follows: (1) the Glaucoma Hemifield Test was outside normal limits; (2) there was a cluster of ≥ 3 nonedge points in a location typical of glaucoma, all of which were depressed on the pattern deviation plot at the $P < 5\%$ level and one of which was depressed at the $P < 1\%$ level; (3) the corrected pattern SD was significant at the $P < 5\%$ level.

LSFG

The effects of topical tafluprost instillation on ONH blood flow were studied using the MBR, a blood-flow parameter in LSFG. The MBR was calculated from the blood-flow map obtained using analysis software provided for LSFG (LSFG analyzer, version 3.0.20.0). After we had identified the margin of the optic disc using an ellipsoidal band by manually, all the positions were saved and used on the same patient for subsequent analyses automatically. The ONH area on the blood-flow map was determined by fitting on ellipsoidal rubber band to the borderline of the ONH. Consecutive MBR measurements were performed 3 times to get an average MBR for each time-point. The changes in MBR were normalized to the baseline value (last measurement before topical tafluprost instillation), and normalized values were compared between the treatment eyes and the fellow control eyes in the same patients.

Statistical Analysis

A paired t test was used to examine differences from the baseline, and repeated-measures analysis of variance and a paired t test were applied to the difference between the 2 eyes. When necessary, Bonferroni correction was used to adjust P values. $P < 0.05$ was considered significant.